UNSTEADY SOLUTION OF A 2D STATOR-ROTOR INTERACTION

Petr Straka
Aeronautical Research and Test Institute, Plc, Prague

Abstract

This contribution describes a 2D unsteady solution of a stator-rotor interaction for a subsonic steam turbine cascade Škoda ST6 and a transonic gas turbine cascade PBS TJ100. The method used for solution is based on the RANS equations coupled with a TNT k-ω turbulence model. The problem is solved by an implicit finite volume method for compressible flow on a structured quadrilateral multiblock chimera grid. Influence of a time discretization (backward Euler's second order scheme vs. Crank's-Nicolson's scheme), a space discretization (2D linear reconstruction: Van Albada's vs. Van Leer's limiter) and a physical model (viscous turbulent vs. inviscid model) on a time behaviour and a spectrum of a forces action is described.

Nomenclature

t_{st}	stator blades pitch	ω	specific dissipation of the kinetic turbulent energy
t	physical time	τ_{ij}	viscous stress tensor
D	pich diameter	$q_x,\ q_y$	heat flux
p_{01}	inlet total pressure	μ	molecular viscosity
p_2	outlet pressure	μ_t	turbulent viscosity
T_{01}	inlet total temperature	$\sigma_k,\ \sigma_\omega$	turbulent model constant
v_{cr}	circumferential speed	$x,\ y$	Cartesian coordinates
α_1	angle of attack	$P_k,\ P_\omega$	production terms
W	state vector	$D_k,\ D_\omega$	destructions terms
$F,\ G$	inviscid fluxes	C_D	cross-diffusion term
$R,\ S$	viscous fluxes	κ	adiabatic exponent
Q	source terms vector	λ	thermal conductivity coefficient
ρ	density	λ_t	turbulent thermal conductivity coefficient
$u,\ v$	velocity vector components	Δt	physical time step
e	tonal energy per unit	$\Delta \tau$	dual time step
p	pressure	$\mathcal{R}$	residuum
T	temperature	n	index of physical time layer
k	turbulent kinetic energy	ν	index of dual time layer

Introduction

This paper deals with the solution of the 2D unsteady flow through a turbine stage. Main object of this work is a study of an influence of various conditions of the simulation (physical model, numerical method) on an unsteady aerodynamics forces.

The solution is done for two different types of geometry. The first is a cylindrical section of the steam turbine stage "ST6" designed by Škoda Power a.s. which works in a subsonic regime. The second type of geometry is a cylindrical section of the gas turbine stage "TJ100" designed by PBS Velká Bíteš a. s. which works in a transonic regime. The other difference between this two types of geometry is a thickness (or radius) of a trailing edge. The cascade TJ100 has much thicker trailing edge of both stator and rotor blades compared with the cascade ST6 which leads (in according with a simulation results) to stalling of flow and generating of a vortex series in a wake of TJ100 cascade blades contrary of the cascade ST6.

A scheme of both types of geometry and parameters of flow is shown in following table:

	ST6	TJ100
geometry		
rpm	4346 min^{-1}	13 054 min^{-1}
stator blades pitch t_{st}	28.798 mm	24,7737 mm
stator : rotor blades	70 : 90	40 : 30
pich diameter D	552 mm	275 mm
inlet total pressure p_{01}	131 100 Pa	130 000 Pa
inlet total temperature T_{01}	328.96 K	318.00 K
angle of attack α_1	0°	0°
outlet pressure p_2	95 380 Pa	46 400 Pa
circumferential speed v_{cr}	125.61 ms^{-1}	187.96 ms^{-1}
fluid	ideal gas	ideal gas

Tab. 1 – *Parameters of the cascades ST6 and TJ100*

Physical and mathematical model

Used model of an unsteady compressible viscous or inviscid flow of an ideal gas is described by the RANS equations coupled with a two-equations TNT $k - \omega$ turbulence model (1) resp. by the Euler equations (from (1) with removing of a viscous terms and a part of the turbulence model).

$$\frac{\partial W}{\partial t} + \frac{\partial F(W)}{\partial x} + \frac{\partial G(W)}{\partial y} - \frac{\partial R(W, \Delta W)}{\partial x} - \frac{\partial S(W, \Delta W)}{\partial y} = Q, \tag{1}$$

where

$$W = [\rho, \rho u, \rho v, \ e, \rho k, \rho \omega]^T \tag{2}$$

is a state vector,

$$F(W) = [\rho u, \rho u^2 + p, \rho uv, u(e + p), \rho uk, \rho u\omega]^T \tag{3}$$

and

$$G(W) = [\rho v, \rho uv, \rho v^2 + p, v(e + p), \rho vk, \rho v\omega]^T \tag{4}$$

are an inviscid fluxes,

$$R(W, \Delta W) = \left[0, \tau_{xx}, \tau_{xy}, u\tau_{xx} + v\tau_{xy} - q_x, (\mu + \sigma_k \mu_t)\frac{\partial k}{\partial x}, (\mu + \sigma_\omega \mu_t)\frac{\partial \omega}{\partial x}\right]^T \tag{5}$$

and

$$S(W, \Delta W) = \left[0, \tau_{xy}, \tau_{yy}, u\tau_{xy} + v\tau_{yy} - q_y, (\mu + \sigma_k \mu_t)\frac{\partial k}{\partial y}, (\mu + \sigma_\omega \mu_t)\frac{\partial \omega}{\partial y}\right]^T \tag{6}$$

are a viscous fluxes and

$$Q = [0, 0, 0, 0, P_k - D_k, P_\omega - D_\omega - C_D]^T \tag{7}$$

is a vector of a source terms. Relation between total energy per unit and pressure is given by state equation as:

$$p = (\kappa - 1)\left[e - \rho(u^2 + v^2)/2\right], \tag{8}$$

where κ is an adiabatic exponent. The viscous stress tensor is given by formula (in an indexical notation with using of the Stokes's relation for both types of the viscosity):

$$\tau_{ij} = (\mu + \mu_t)\left(\frac{\partial u_i}{\partial x_j} + \frac{\partial u_j}{\partial x_i} - \frac{2}{3}\delta_{ij}\frac{\partial u_k}{\partial x_k}\right) - \frac{2}{3}\delta_{ij}\rho k. \tag{9}$$

The molecular viscosity is given by the Sutherland's law:

$$\frac{\mu}{\mu_0} = \left(\frac{T}{T_0}\right)^{3/2}\frac{T_0 + S}{T + S}, \tag{10}$$

where $T_0 = 273.15$ K and $S = 110.3$ K. The turbulent viscosity is given by formula:

$$\mu_t = \frac{\rho k}{\omega}. \tag{11}$$

The heat flux in (5) and (6) is given by the Fourier's law:

$$q_j = -(\lambda + \lambda_t)\frac{\partial T}{\partial x_j}, \tag{12}$$

where λ is a thermal conductivity coefficient and λ_t is a turbulent thermal conductivity coefficient. The terms P_k resp. P_ω in (7) are the production and D_k resp. D_ω are the destruction of the turbulent kinetic energy and the specific dissipation of the kinetic turbulent energy respectively, C_D is a cross-diffusion term [1].

Numerical method

The governing equations (1) are discretized on a structured quadrilateral multiblock grid (with an implementation of a block overlapping) using a cell-centered finite-volume technique and solved through full implicit time-marching scheme. The part of the two-equations turbulence model is solved separately from the RANS equations. The inviscid fluxes of the RANS equations are solved by the Osher's-Solomon's scheme [2], the viscous fluxes are solved by a central scheme using a dual grid. The convective terms of the turbulence model equations are solved by the Steger's-Warming's upwind scheme [2], the diffusive terms are solved by the central scheme using the dual grid.

The 2D linear reconstruction technique with the Van Albada's or Van Leer's limiter [2] is used to to obtain of higher precision order in a space whereas the influence of the type of limiter on the results is discussed in following paragraphs.

The backward Euler's second order scheme (13) and the Crank's-Nicolson's scheme (14) are used for a time discretization.

$$\frac{3W^{n+1} - 4W^n + W^{n-1}}{2\Delta t} = \mathcal{R}(W^{n+1}), \tag{13}$$

$$\frac{W^{n+1} - W^n}{\Delta t} = \frac{1}{2}\left[\mathcal{R}(W^{n+1}) + \mathcal{R}(W^n)\right], \tag{14}$$

where $\mathcal{R}$ is a residuum, Δt is a physical time step and n is an index of a physical time layer. Both schemes are realized through a time fixing method in a dual time:

$$\frac{3}{2}\frac{W^{n+1,\nu+1} - W^{n+1,\nu}}{\Delta \tau} = -\frac{3W^{n+1,\nu} - 4W^n + W^{n-1}}{2\Delta t} + \mathcal{R}(W^{n+1,\nu+1}) \tag{15}$$

for the backward Euler's second order scheme or

$$\frac{W^{n+1,\nu+1} - W^{n+1,\nu}}{\Delta \tau} = -\frac{W^{n+1,\nu} - W^n}{\Delta t} + \frac{1}{2}\left[\mathcal{R}(W^{n+1,\nu+1}) + \mathcal{R}(W^n)\right] \tag{16}$$

for the Crank's-Nicolson's scheme. In (15) and (16) there $\Delta \tau$ is a dual time step and ν is an index of a dual time layer. The dual time step $\Delta \tau$ is set with respect to stability and convergence of the iterative proces in the dual time whereas the physycal time step Δt is restricted only by a physycal phenomenon (e.g. the circumferential speed in this contribution). The time fixing method in the dual time for both (15) and (16) schemes proceeds in folowing steps:

1. set $W^{n+1,0} = W^n$,
2. solve $W^{n+1,\nu+1}$ from $W^{n+1,\nu}$ up to obtain a stady state W^{n+1,ν^*} (or to achiving of a maximum number of the dual iterations),
3. set $W^{n+1} = W^{n+1,\nu^*}$.

The other possibility is to use of a method with a priori determined number of the dual iterations [3]. For choice of $\Delta \tau = \frac{3}{2}\Delta t$ we can rewrite equation (15) to form:

$$\frac{3}{2}\left(W^{n+1,\nu+1} - W^{n+1,\nu}\right) = -\frac{3W^{n+1,\nu} - 4W^n + W^{n-1}}{2} + \Delta t\mathcal{R}(W^{n+1,\nu+1}). \tag{17}$$

In (17) the physical time step Δt must be set with respect to both physycal restriction and stability and convergence restriction. By using (17) with performance of the stability and convergence condition to obtain the second order of accuracy in a time two dual iterations are enough [3].

Alike it is possible to use the Crank's-Nicolson's scheme with a priori determined number of the dual iterations. For choice of $\Delta \tau = \Delta t$ we can rewrite equation (16) to form:

$$W^{n+1,\nu+1} - W^{n+1,\nu} = -\left(W^{n+1,\nu} - W^n\right) + \frac{\Delta t}{2}\left[\mathcal{R}(W^{n+1,\nu+1} + \mathcal{R}(W^n))\right]. \quad (18)$$

It is possible to use the physical time step Δt in (18) the same as in (17).

The influence of used scheme (backward Euler's or Crank's-Nicolson's) and used iterative method in the dual time – the time fixing method in the dual time (15) and (16) or the method with a priori determined number of the dual iterations (17) and (18) – much like the influence of the choice of the physical time step Δt on the results is tested and discussed in following paragraphs.

Boundary conditions

The relationship of number of stator and rotor blades was modified for simulation demand from real number to 70:90 for ST6 cascade resp. 30:40 for TJ100 cascade. It makes possible to use a periodically repeating domain containing seven stator and nine rotor blades for the ST6 cascade resp. three stator and four rotor blades for the TJ100 cascade.

The scheme of the computational domain with marked types of a boundary conditions is shone in Fig. 1. Values of the prescribed quantities are mentioned in Tab. 1. The total pressure p_{01}, the total temperature T_{01} and the angle of attack α_1 are prescribed at the inlet boundary. The integral of the static pressure p_2 is prescribed at the outlet boundary. Continuity of the static pressure and desity is prescribed at the interface between stator and rotor part (with respect to the time dependent mutual shift of the rotor blades to the stator blades). The velocity vector at the interface respects the circumferential speed v_{cr}.
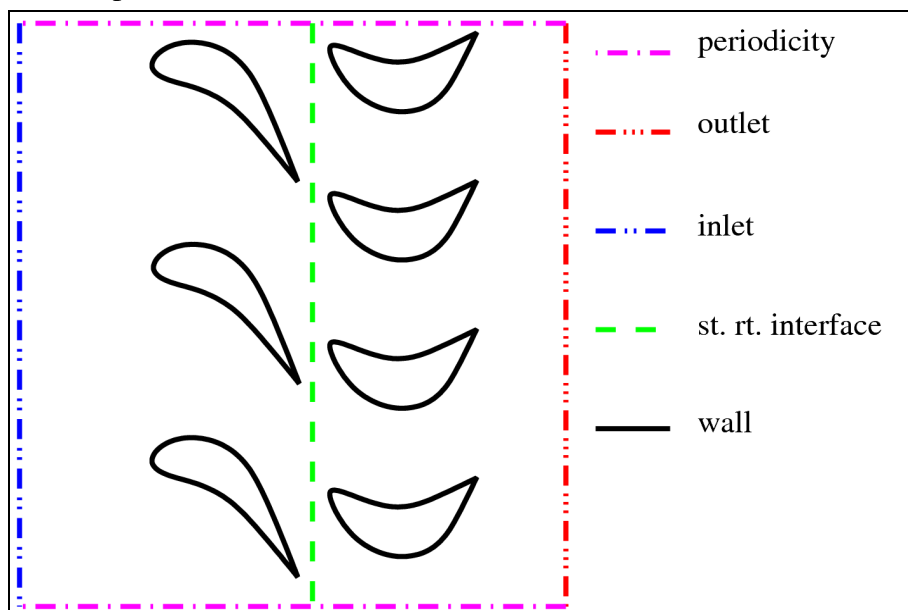
Fig. 1 – *Scheme of a computational domain*

Computational grid

The structured quadrilateral multiblock grid with an implementation of a block overlapping (so-called chimera grid) is used for discretization of the computational domain. The grid is combined from the "O"-type blocks around the blades and "H"-type basic blocks (see fig. 2 and fig. 3).
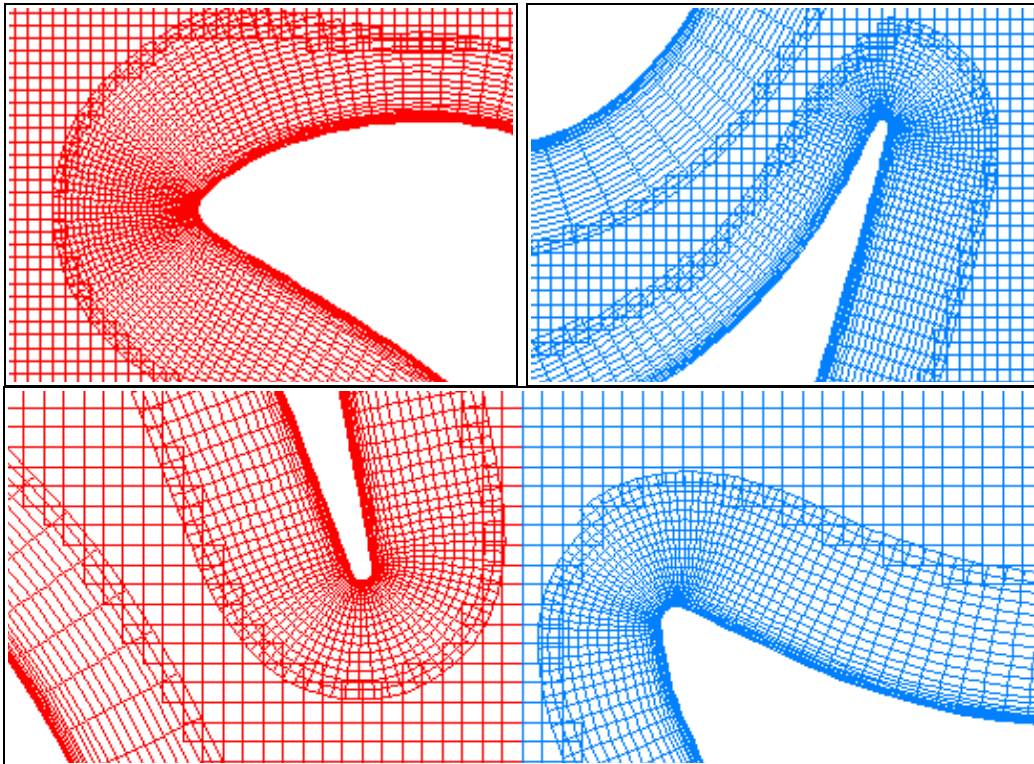
Fig. 2 – *Computational grid for the ST6 cascade, red – stator part, blue – rotor part*
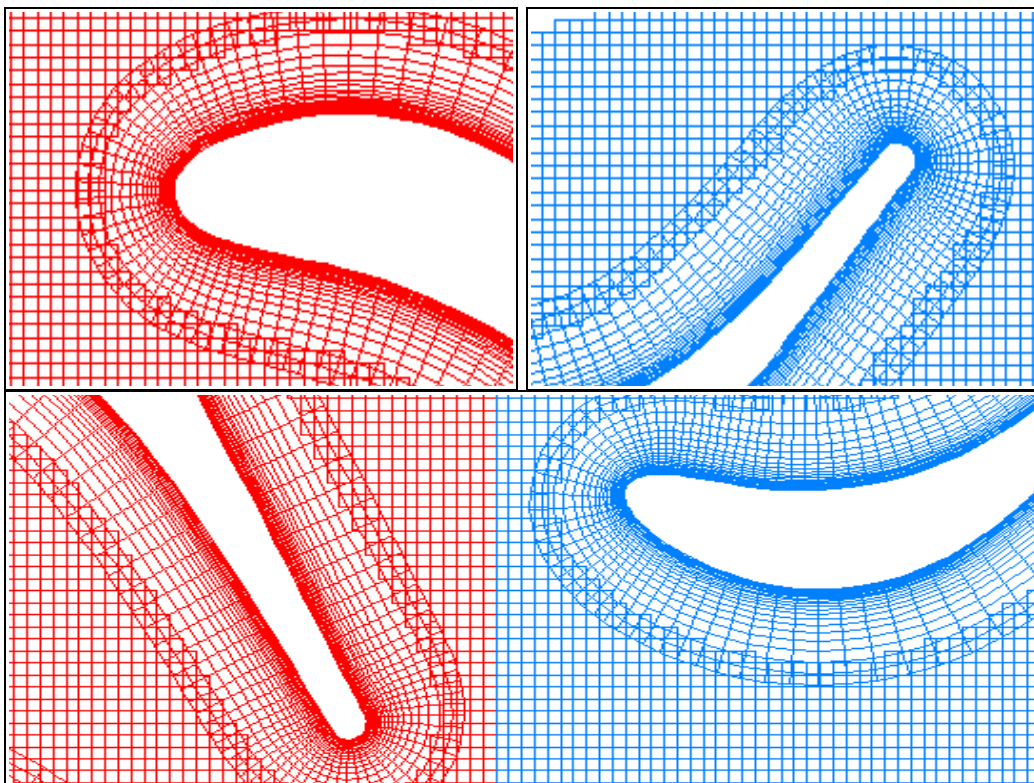
Fig. 3 – *Computational grid for the TJ100 cascade, red – stator part, blue – rotor part*

Results and discussion

A character of a flowfields in a static temperature isolines form in the blades ST6 and TJ100 we can compar in Fig. 4. We can see, that contrary to the cascade ST6 where the trailing edges are relatively sharp in the cascade TJ100 in consequence of thick trailing edges the vortex series behind the stator blades is generated. Of course a physical correctness of this effect is controversial in relation to used physical model and numerical method (namely the TNT $k - \omega$ turbulence model and computational grid). However a presence of a higher frequence effect in the flow field make possible to check an ability of different variants of used physical model and numerical method to represent the higher frequence effect.

ST6   TJ100
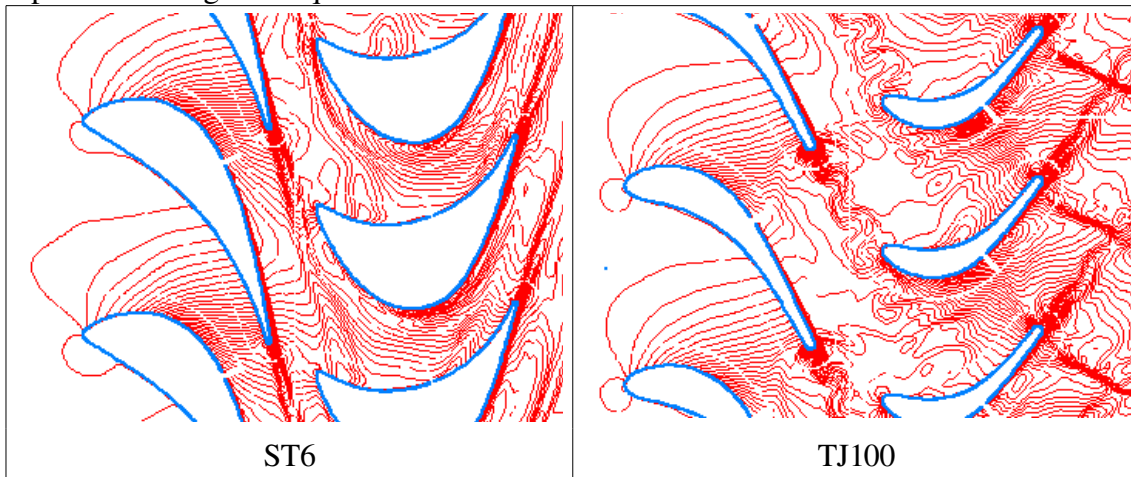
Fig. 4 – *Flow field – static temperatute isolines, left: ST6cascade, right: TJ100 cascade*

The properties of used models are presented on a time behaviour of an action of force $F_x(t)$ and $F_y(t)$ at stator and rotor blades and their frequency spectrum. The influence of the physycal model – viscous tyrbulent and inviscid model is presented in Fig. 5 for the cascade ST6 and Fig. 6 for the cascade TJ100. In both cases the scheme (17) with 2016 physical steps per period for ST6 and 1008 steps per period fos TJ100 was used. We can see a slightly shift of the time behaviour of the forces obtained by the inviscid model against the turbulent model in the cascade ST6 however the spectrums of both models are almost identical (Fig. 5). In the cascade TJ100 we can see slightly increasing of amplitude of higher frequency effect and shift this frequency (from 38.000 Hz to 45.000 Hz) for inviscid model against to turbulent model, lower frequency effect are by both models checked almost identycaly.
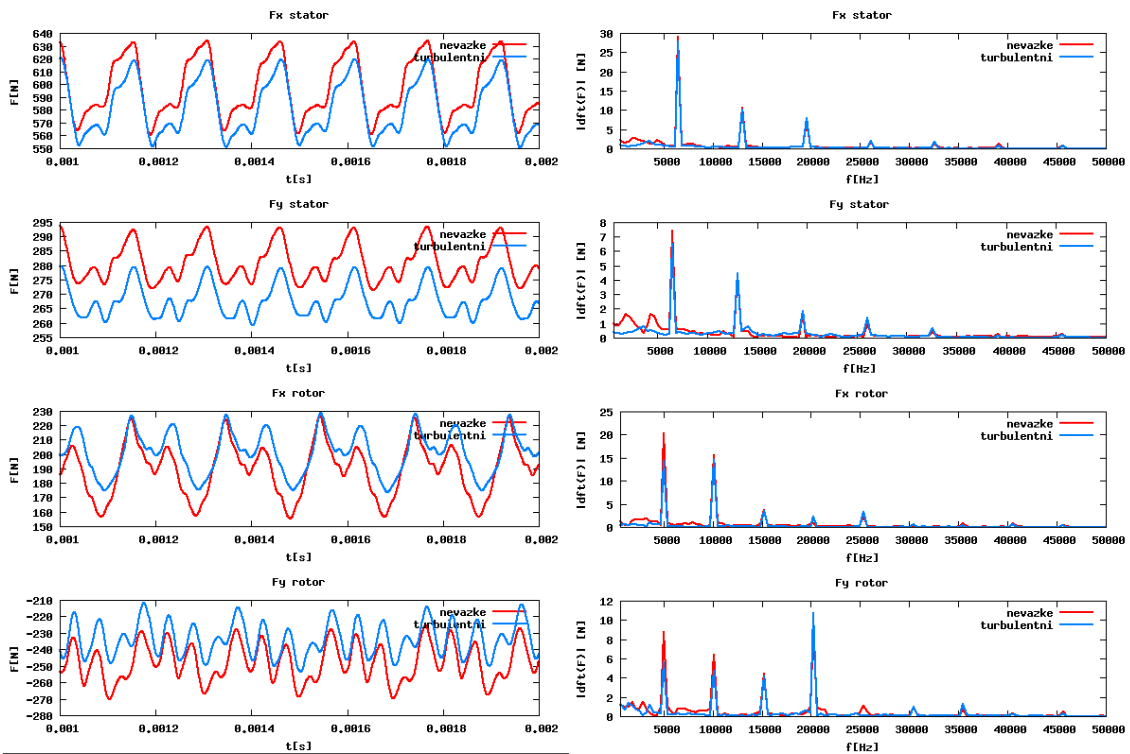
Fig. 5 – *Comparison of viscous turbulent and inviscid model in the cascade ST6,*
red: inviscid, blue: viscous turbulent
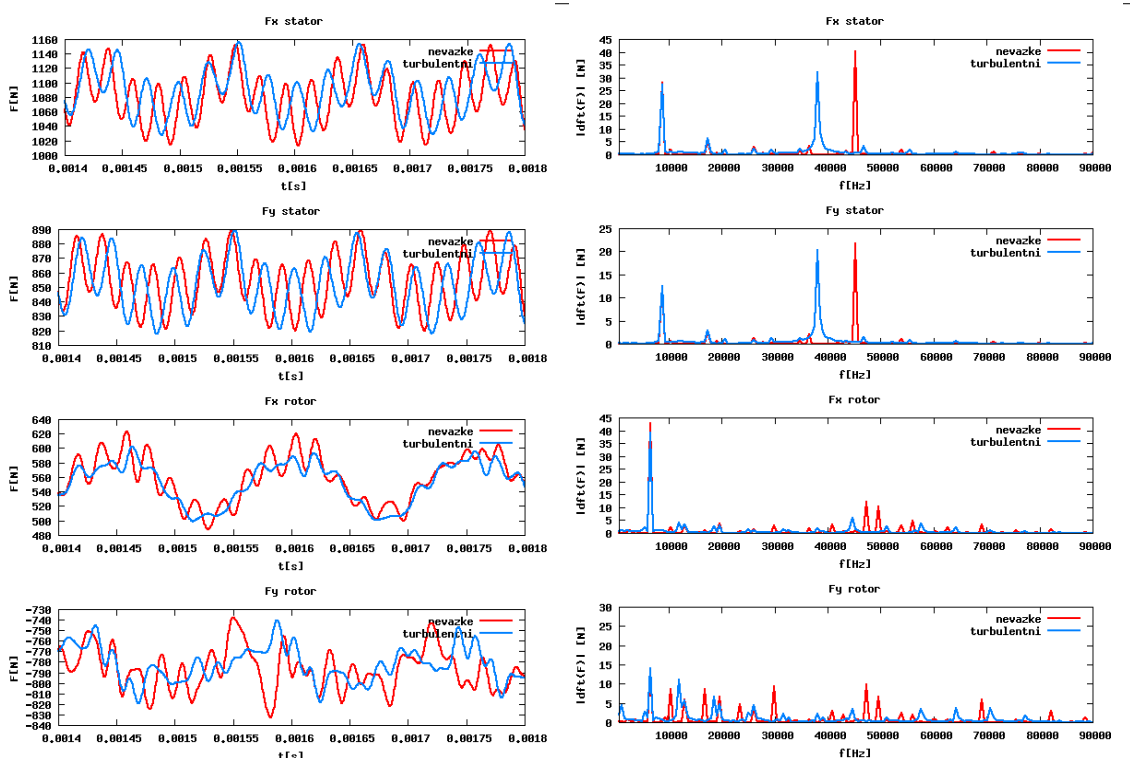
Fig. 6 – *Comparison of viscous turbulent and inviscid model in the cascade TJ100, red:*
inviscid, blue: viscous turbulent

The influence of used type of limiter (Van Albada's or Van Leer's) in 2D linear reconstruction technique is presented in Fig. 7 in the cascade TJ100. The scheme (17) with 1008 physycal steps per period and the inviscid model are used in this case. We can see, that the spectrum in both cases is practically the same, but we can recognize some dissimilarities in the time behaviours although the difference between both used methods is very small. This example illustrates a dependence of time behaviour of quantities in unsteady cases on the space discretization.
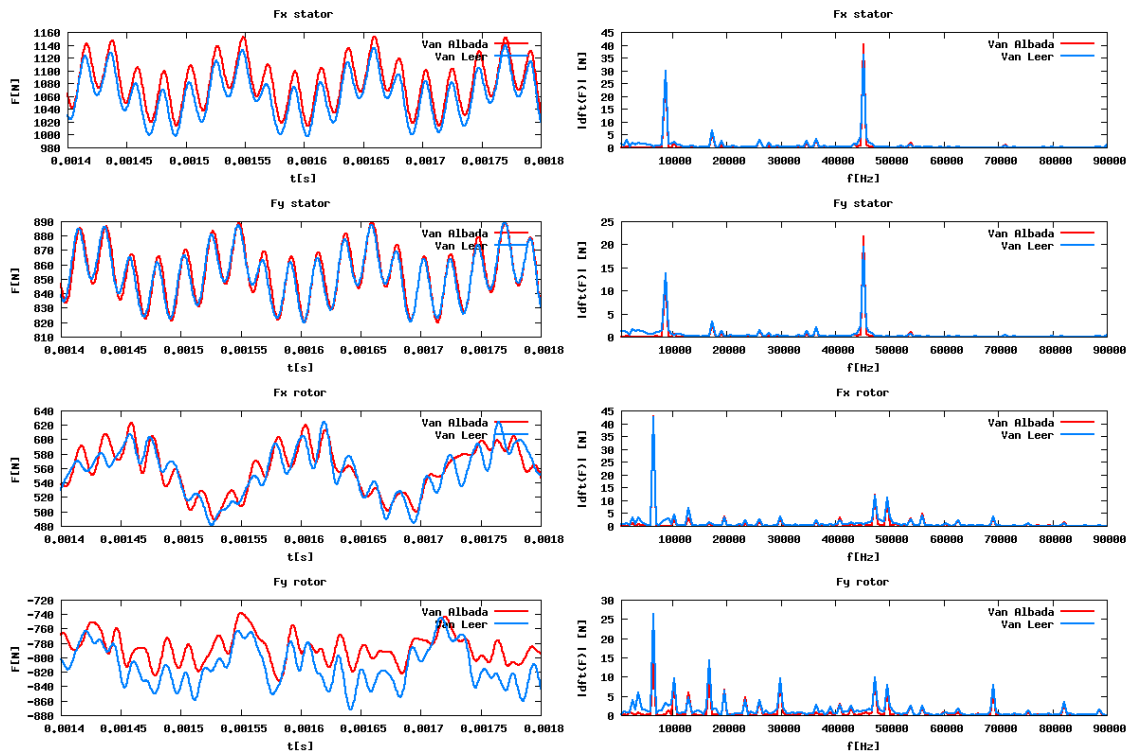
Fig. 7 – *Influence of type of limiter, red: Van Albada's limiter, blue: Van Leer's limiter*

The differece between the second order backward Euler's scheme and the Crank's-Nicolson's scheme is presented in Fig. 8 in the cascade TJ100. The schemes (17) and (18) with 1008 physycal steps per period and the inviscid model are used in this case. We can see that differences between this two schemes are minimal in both time and frequence domain. The Euler's scheme is a bit more robust in start of solution than Crank's – Nicolson's scheme.
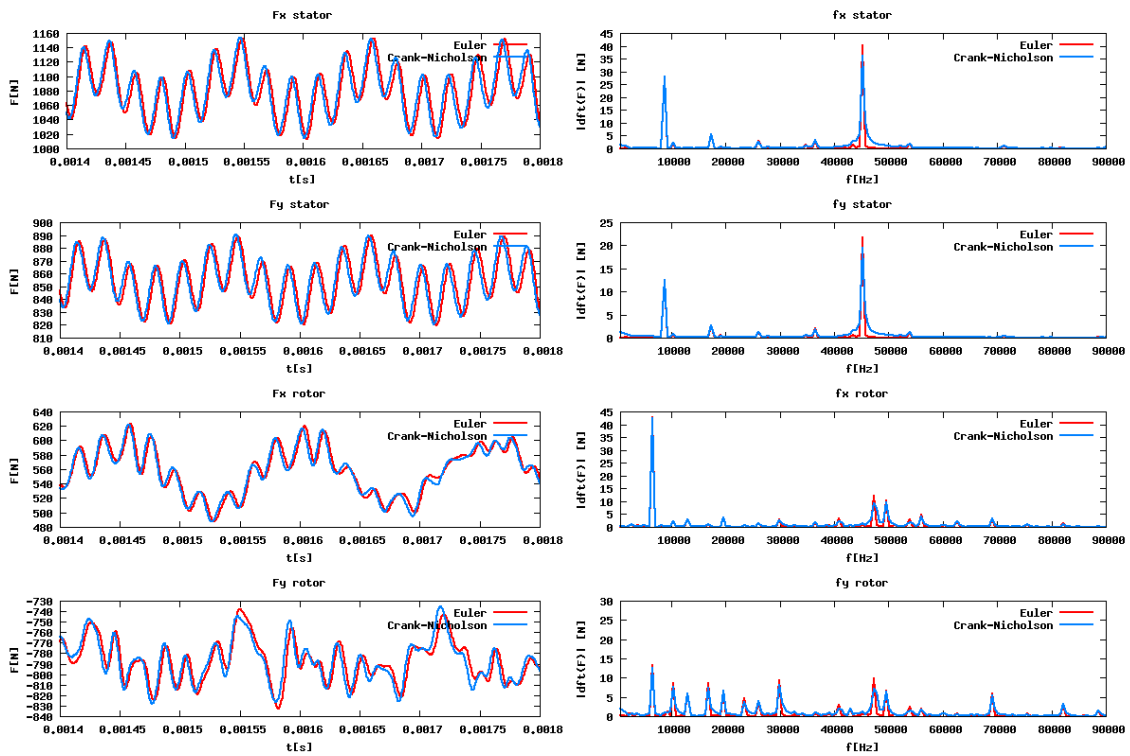
Fig. 8 – *Influence of type of time discretization, red: second order backward Euler's scheme, blue: Crank's-Nicolson's scheme*

The influence of choise of the physical time step Δt which is joint with the circumferential speed v_{cr} and the number of the physycal steps per period is presented in Fig. 9 for the cascade ST6 with using of the viscous turbulence model and the Euler's schemes (15) or (17) and in Fig. 10 for the cascade TJ100 with using of the inviscid model and the Crank's – Nicolson's schemes (16) or (18). In the cascade ST6 was used 2016 physical steps per period with the Euler's scheme in form (17) or 63 physical steps per period with the Euler's scheme in form (15) with restriction to maximum 30 dual iterations. In the cascade TJ100 was used 1008 physycal steps per period with the Crank's – Nicolson's scheme in form (18) or 108 physical steps per period with the Crank's – Nicolson's scheme in form (16) with restriction to maximum 30 dual iterations. Using of lower number of the physical steps per period don't leads to acceleration of solution (high number of the dual iterations) but it leads to losse of the accuracy in time. In Fig. 9 we can see that by using of lower number of the physical steps per period is checked only first major frequence (and partially second major frequence for the rotor blades). In Fig. 10 we can see that by using of lower number of the physical steps per period are high frequence effect shifted from 45.000 Hz (for invoscid model) to 24.000 Hz.
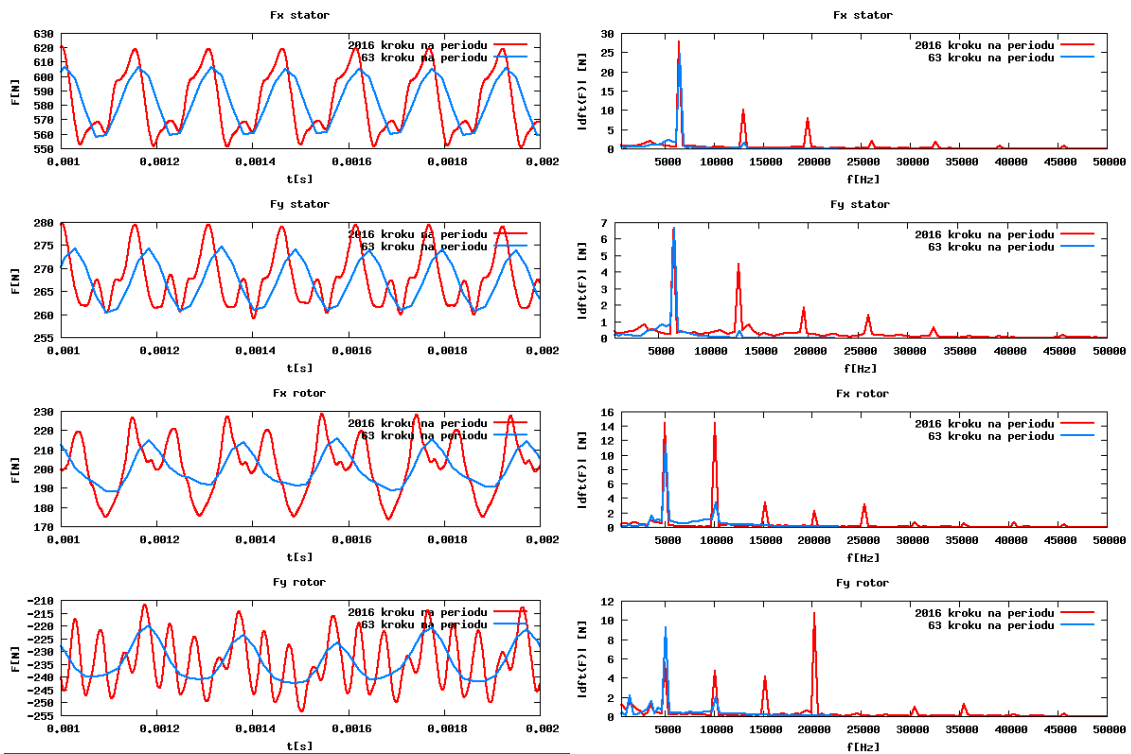
Fig. 9 – *Influence of physical time step Δt in cascade ST6, red: 2016 steps per period, blue: 63 steps per period*
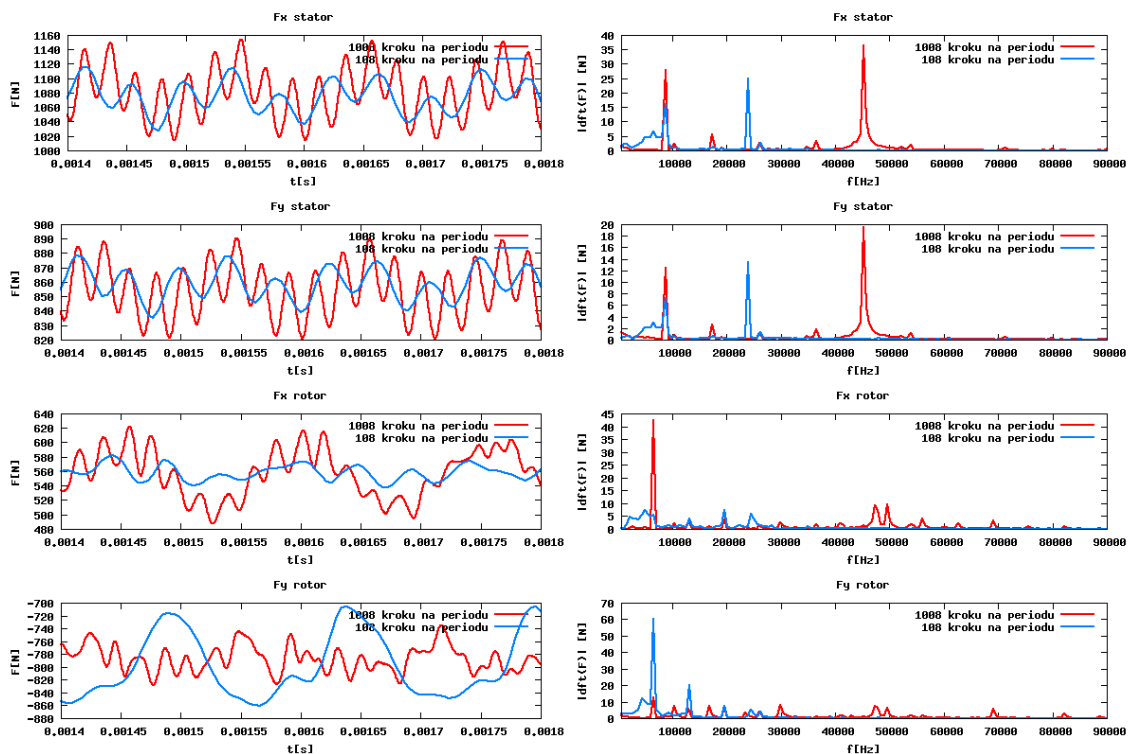
Fig. 10 – *Influence of physical time step Δt in cascade TJ100, red: 1008 steps per period, blue: 108 steps per period*

Conclusion

By virtue of the simulations of the unsteady stator – rotor interaction in the cascades ST6 and TJ100 by using of various physical models and modifications of numerical methods we can say that using of the iviscid model leads to slightly shift of the mean values of the forces against results obtained by the turbulent model in the cascade ST6. Another result of using of the inviscid model if slightly increase of the frequence of the high-frequence effect in the cascade TJ100.

The results obtained by using of the Van Albada's limiter and the Van Leer's limiter are similar, but this example illustrates a dependence of time behaviour of quantities in unsteady cases on the space discretization.

The second order backward Euler's scheme and the Crank's-Nicolson's scheme give almost the same results, but the Euler's scheme is a bit more robust in start of solution than Crank's – Nicolson's scheme.

Using of lower number of the physical steps per period don't leads to acceleration of solution (high number of the dual iterations) but it leads to losse of the accuracy in time.

Acknowledgement

References

[1] Kok, J. C.: Resolving the Dependence on Freestream Values for $k - \omega$ Turbulence Model, AIAA Journal, Vol. 38, No. 7, 2000.

[2] Feistauer M., Felcman J., Straškraba I.: Mathematical and Computational Methods for Compressible Flow. Oxford University Press, 2003.

[3] Fořt J., Fürst J., Halama J., Kozel K., Louda P., Sváček P.: Numerické řešení nestacionárního proudění v turbínovém stupni ST6. Report FS ČVUT 201-08-155, Prague 2008.

[4] Straka P.: Výpočet nestacionárního proudění v turbínovém stupni ST6. Report VZLÚ R-4476, Prague 2008.